

Journal of Visualized Experiments

A neonatal imaging model of Gram-negative bacterial sepsis

--Manuscript Draft--

| | |
|--|--|
| Article Type: | Methods Article - JoVE Produced Video |
| Manuscript Number: | JoVE61609R1 |
| Full Title: | A neonatal imaging model of Gram-negative bacterial sepsis |
| Section/Category: | JoVE Immunology and Infection |
| Keywords: | Bioluminescence; intravital imaging; E. coli; subscapular inoculation; neonates; sepsis; inflammation; cytokines |
| Corresponding Author: | Cory Robinson, Ph.D. West Virginia University Morgantown, WV UNITED STATES |
| Corresponding Author's Institution: | West Virginia University |
| Corresponding Author E-Mail: | cory.robinson1@hsc.wvu.edu |
| Order of Authors: | Brittany G. Seman, Ph.D. Jessica M. Povroznik Jordan K. Vance Travis W. Rawson Cory M. Robinson |
| Additional Information: | |
| Question | Response |
| Please indicate whether this article will be Standard Access or Open Access. | Standard Access (US\$2,400) |
| Please indicate the city, state/province, and country where this article will be filmed . Please do not use abbreviations. | Morgantown, West Virginia, USA |

TITLE:

A Neonatal Imaging Model of Gram-Negative Bacterial Sepsis

AUTHORS AND AFFILIATIONS:

Brittany G. Seman^{1*}, Jessica M. Povroznik^{1,2*}, Jordan K. Vance¹, Travis W. Rawson¹, Cory M. Robinson^{1,2}

¹Department of Microbiology, Immunology, & Cell Biology, West Virginia University School of Medicine, Morgantown, West Virginia, USA

²Vaccine Development Center at West Virginia University Health Sciences Center, Morgantown, West Virginia, USA

*These authors contributed equally.

Corresponding Author:

Cory M. Robinson (cory.robinson1@hsc.wvu.edu)

Email Addresses of Co-authors:

Brittany G. Seman (brittany.seman@hsc.wvu.edu)

Jessica M. Povroznik (jessica.povroznik@hsc.wvu.edu)

Jordan K. Vance (jkh0003@mix.wvu.edu)

Travis W. Rawson (twr0001@mix.wvu.edu)

KEYWORDS:

bioluminescence, intravital imaging, *E. coli*, subscapular inoculation, neonates, sepsis, inflammation, cytokines

SUMMARY:

Infection of neonatal mice with bioluminescent *E. coli* O1:K1:H7 results in a septic infection with significant pulmonary inflammation and lung pathology. Here, we describe procedures to model and further study neonatal sepsis using longitudinal intravital imaging in parallel with enumeration of systemic bacterial burdens, inflammatory profiling, and lung histopathology.

ABSTRACT:

Neonates are at an increased risk of bacterial sepsis due to the unique immune profile they display in the first months of life. We have established a protocol for studying the pathogenesis of *E. coli* O1:K1:H7, a serotype responsible for high mortality rates in neonates. Our method utilizes intravital imaging of neonatal pups at different time points during the progression of infection. This imaging, paralleled by measurement of bacteria in the blood, inflammatory profiling, and tissue histopathology, signifies a rigorous approach to understanding infection dynamics during sepsis. In the current report, we model two infectious inoculums for comparison of bacterial burdens and severity of disease. We find that subscapular infection leads to disseminated infection by 10 h post-infection. By 24 h, infection of luminescent *E. coli* was abundant in the blood, lungs, and other peripheral tissues. Expression of inflammatory

cytokines in the lungs is significant at 24 h, and this is followed by cellular infiltration and evidence of tissue damage that increases with infectious dose. Intravital imaging does have some limitations. This includes a luminescent signal threshold and some complications that can arise with neonates during anesthesia. Despite some limitations, we find that our infection model offers an insight for understanding longitudinal infection dynamics during neonatal murine sepsis, that has not been thoroughly examined to date. We expect this model can also be adapted to study other critical bacterial infections during early life.

INTRODUCTION:

Bacterial sepsis is a significant concern for neonates that exhibit a unique immune profile in the first days of life that does not provide adequate protection from infection¹. Neonatal sepsis continues to be a significant U.S. healthcare problem accounting for greater than 75,000 cases annually in the U.S alone². To study these infections in depth, novel animal models that recapitulate aspects of human disease are required. We have established a neonatal mouse infection model using *Escherichia coli*, O1:K1:H7³. *E. coli* is the second leading cause of neonatal sepsis in the U.S., but responsible for the majority of sepsis-associated mortality^{4,5}. However, it is the leading cause when pre-term and very-LBW babies are considered independently⁵. The K1 serotype is most frequently associated with invasive bloodstream infections and meningitis in neonates^{6,7}. Currently, there are no other treatment options beyond antibiotics and supportive care. Meanwhile, rates of antibiotic resistance continue to rise for many pathogenic bacteria, with some strains of *E. coli* resistant to a multitude of antibiotics commonly used in treatment⁸. Thus, it is imperative that we continue to generate methods to study the mechanisms of sepsis and the host response in neonates. These results can help to improve upon current treatments and infection outcomes.

The immune state of neonates is characterized by both phenotypic and functional differences compared to adults. For instance, elevated levels of anti-inflammatory and regulatory cytokines, such as interleukin (IL)-10 and IL-27, have been shown to be produced by cord blood-derived macrophages and are present at greater levels in the serum of murine neonates⁹⁻¹¹. This is consistent with lower levels of IFN- α , IFN- γ , IL-12, and TNF- α that are frequently reported from neonatal cells compared with adult counterparts¹⁰. Additionally, the neonatal immune system is skewed toward a Th2 and regulatory T cell response as compared to adults¹². Elevated numbers of neutrophils, T cells, B cells, NK cells, and monocytes are also present in neonates, but with significant functional impairments. This includes defects in expression of cell surface markers and antigen presentation that suggest immaturity¹³⁻¹⁵. Additionally, neonatal neutrophils are significantly deficient in their ability to migrate to chemotactic factors¹⁶. Myeloid-derived suppressor cells (MDSCs) are also found at elevated levels in neonates and recently shown to be a source of IL-27¹¹. MDSCs are highly suppressive toward T cells¹⁷. Collectively, these data demonstrate limitations in neonatal immunity that lend to increased susceptibility to infection.

To study the progression of the bacterial burden and dissect protective host immune responses during neonatal sepsis, we have developed a novel infection model. Neonatal mice at days 3-4 of life are difficult to inject in the intraperitoneal space or tail vein. In our model, day 3 or 4

pups are administered the bacterial inoculum or PBS subcutaneously into the scapular region. A systemic infection develops and using luminescent *E. coli* O1:K1:H7, we can longitudinally image individual neonatal mice to follow the disseminated bacterial burden in peripheral tissues. This is the first reported model to utilize intravital imaging to understand the kinetics of dissemination of bacteria during sepsis in murine neonates³.

Here, we describe a protocol to induce septic *E. coli* infections in neonatal mice³. We describe how to prepare the bacterial inoculum for injection, and how to harvest tissue for assessment of pathology, measurement of inflammatory markers by gene expression analysis, and enumeration of the bacterial burden. In addition, the use of luminescent *E. coli* for intravital imaging of infected neonates and quantification of bacterial killing by neonatal immune cells is also described. These protocols may also be adapted to study other important bacterial infections in neonates. The data presented here represents an overall novel approach to understanding infection dynamics in a translatable neonatal sepsis model.

PROTOCOL:

All procedures were approved by the West Virginia Institutional Animal Care and Use Committees and conducted in accordance with the recommendations from the Guide for the Care and Use of Laboratory Animals by the National Research Council¹⁸.

1. Preparation of Bacterial Inoculum

1.1 Streak a Tryptic soy agar (TSA) plate with an inoculating loop for isolation of a single colony from a freezer stock of *E. coli* O1:K1:H7-*lux* that stably expresses luciferase and carries kanamycin resistance³. Incubate overnight at 37 °C.

1.2 The following day allow Luria broth (LB) to come to room temperature (25 °C) in a biosafety cabinet.

1.3 Under a biosafety cabinet hood, identify a single colony from the streaked plate and inoculate it in 3 mL of LB supplemented with kanamycin (30 µg/mL). Incubate overnight at 37 °C with shaking (220 rpm). This is the starter culture.

1.4 Dilute the starter culture 1:100 into a fresh 3 mL of LB under a biosafety cabinet hood and return it to the incubator for 2-3 h at 37 °C with shaking (220 rpm). This is the stock culture.

1.5 Read the optical density (OD) of both the blank and stock culture at 600 nm using a spectrophotometer. Add 100 µL of LB (containing no bacteria) into one well of a 96 well flat bottom assay plate; this is the blank. Then add 100 µL from the stock culture to a separate well. Repeat for two additional replicates. The absorbance is read using a plate reader.

1.6 Subtract the blank absorbance from the stock culture absorbance value (the OD value) and compare to a previously generated and validated growth curve to determine an approximation of the bacterial density in the stock culture for the preparation of infectious dose.

1.7 Generate target inoculums depending on the research question. Target inoculum of 2×10^6 (low) and 7×10^6 (high) colony-forming units (CFUs) per mouse (/mouse) were used for this study.

1.7.1. Divide the target dose per mouse ($Dose_T$) by the estimated concentration of bacteria in the stock culture (Stock) to get the volume of bacteria needed from the stock tube (V_S).

1.7.2. Multiply V_S by the number of mice (N_M) that need to be infected along with enough for 5-10 extras for the total amount of bacteria required for the infection plus 5-10 additional doses. Remove this volume from the stock tube and add it to a new centrifuge tube.

1.7.3. Use the equation below:

$$\begin{aligned} Dose_T / Stock &= V_S \times N_M \\ &= \text{total volume (VT) of bacteria to be removed from the stock tube.} \end{aligned}$$

1.8 Centrifuge the bacteria at $2,000 \times g$ for 5 min at 4°C and resuspend the bacterial pellet in 50 μL of PBS (pH 7.2-7.6) per mouse to be infected (e.g., for 10 doses of 2×10^6 bacteria each dose, the pellet of 2×10^7 bacteria would be resuspended in 500 μL PBS). Again, it is recommended to prepare more inoculum than is needed. Prepare an equal volume of PBS only for control inoculations. Maintain the infectious inoculum and PBS control on ice until infection.

1.9 Perform seven ten-fold serial dilutions into PBS in a 96 well plastic bottom dilution plate, and plate 25 μL of the dilutions in duplicate onto quadrant TSA plates supplemented with kanamycin (30 $\mu\text{g}/\text{mL}$) to enumerate the actual amount of bacteria administered. Incubate at 37°C overnight for colony formation prior to enumeration.

2. Animal identification

2.1 Arrange a sufficient number of breeding pairs such that litters may be synchronized for age-matched pups. Age variability of ± 1 day is acceptable.

2.2 Identify a pregnant C57BL/6 female mouse and monitor for birth of the litter in advance of the planned experiment to accurately determine age.

2.3 To distinguish between control and infected 3- or 4-day old pups, use a pair of small, fine-tipped, iris scissors to snip the ends of the tails of the control pups only. The infected pups do not receive tail snips. Before cutting the tail, disinfect the skin with a cotton ball doused in 70% ethanol. Apply pressure to the end of the tail with a cotton ball or gauze as needed.

NOTE: This procedure is performed under a biosafety cabinet hood. A tail snip of approximately $1/8$ of an inch is sufficient.

2.4 To identify pups within the control and infected groups, use a 1 mL insulin syringe with a 28 G x ½" permanent needle to tattoo the tails of the pups. Before tattooing, disinfect the skin with a cotton ball doused in 70% ethanol. This procedure is performed under a biosafety cabinet hood.

2.5 To tattoo the tail, apply animal tattoo ink to the tip of the needle. Next, carefully restrain the pup with one hand, with their tail fully exposed. Gently insert the needle under the skin, while maintaining a superficial level of depth, and move the needle parallel with the skin a few millimeters until a small marking, or dot, has been created. Wait a few seconds before slowly removing the needle from under the skin, to avoid excess ink releasing from under the skin.

2.6 Apply pressure to the wound with a cotton ball or gauze as needed. Remove excess tattoo ink on the surface of the skin with 70% ethanol.

2.7 Repeat this process with subsequent mice in the infected and control groups, while adding an additional dot with each successive pup tattooed (e.g., pup 1 will have 1 dot on their tail, pup 2 will have two dots on their tail, etc.).

NOTE: For an additional layer of identification, it is recommended to use separate colors of animal tattoo ink for the control and infected groups.

3. Subscapular inoculation

NOTE: For this study, 2 experiments were performed with a low-dose and high-dose group designated for each experiment. In the first experiment, 7 pups were given the low dose inoculum (4 pups were used as controls), and 5 pups from a separate litter were given the high dose (3 pups were used as controls). The pups from experiment 1 provided data for only the 24 h timepoint. In the second experiment, 8 pups were given the low dose inoculum (2 pups were used as controls), and 6 pups were given the high dose inoculum (2 pups were used as controls). Pups from experiment 2 provided data for the 0, 10, and 24 h timepoints.

3.1 Age match pups ≤ 1 day. Assign each litter as either a low dose or a high dose litter. Within a litter randomly assign pups as a control or infected pup.

3.2 On day 3 or 4 postnatal, record weights of all pups prior to inoculation with *E. coli-lux* or the PBS control. Separate the dam from the pups during this time to ensure they are not moved during the infection.

3.3 Within a biosafety cabinet using an insulin needle, aspirate either PBS or the *E. coli-lux* inoculum. For this work, inoculums of 2×10^6 and 7×10^6 CFUs per mouse were used. Keep both infectious inoculum and PBS on ice until administration via subscapular injection.

3.4 Place the neonate on a clean surface in the biosafety cabinet hood and raise the skin at the nape of the neck as if to scruff the pup.

3.5 In the space now created between the skin and the muscle of the animal, insert the needle, bevel up, just beneath the skin and inject 50 μ L of PBS or *E. coli-lux*. Simultaneously release the pinched portion of skin to prevent injection backflow.

3.6 Remove the needle slowly and with care. Place pups back with dams after injections are finished.

NOTE: Due their anatomical stage in development, it is technically challenging to administer a tail vein or intraperitoneal injection to neonatal pups at day 3-4. Thus, the subscapular infection route was chosen for this study due to the ease of execution.

4. Evaluation of disease and endpoint criteria

4.1 Monitor the pups twice daily throughout the duration of infection. Note any abnormalities in appearance.

4.2 Record weights as an objective measurement of morbidity.

4.3 In addition to weight changes, test the ability of the pups to right themselves by positioning the neonate on the dorsal side. Sick animals will be unable to turn over to the ventral side and onto the feet or will complete this action with difficulty.

4.4 Check for the following to mark the animals close to endpoint criteria: less than 85% of normal body weight; decreased movement and inability to right themselves; discoloration of the skin and amore grey or transparent appearance as opposed to pink; feeling cool to the touch, indicative of decreased body temperature and hemorrhagic bruising along the sides, also indicative of advance illness.

NOTE: If the neonates have failed to gain weight over two days and fit any of the descriptions in steps 4.4, they have met endpoint criteria. Pups that receive the high dose often meet endpoint criteria by 24 h. Control pups within the low and high dose litters will be euthanized at the same time to allow for comparative analysis between the control and experimental groups. Proceed to the euthanasia section below.

5. In vivo imaging of bacterial burden

5.1 Use a microCT imager and software for imaging and subsequent analysis.

NOTE: Pup skin color does not impact imaging quality.

5.2 Place the cage with *E. coli-lux*-infected neonatal mice and dam into a BSL-2 level laminar flow hood. Remove mice to be imaged, and place into a transparent isoflurane chamber within

the hood. It is recommended to start with uninfected controls to gauge the amount of isoflurane needed.

5.3 Open the software on the computer attached to the microCT. Initialize the system and wait for the CCD temperature to lock at 37 °C.

5.4 Turn the isoflurane vaporizer on and adjust the dial to 5% isoflurane flow. Keep mice in the chamber with this isoflurane mixture for 20-30 s until they stop moving; longer or shorter anesthesia exposure times may be needed for some mice. Once mice stop moving, they are sufficiently anesthetized, and can be imaged.

5.5 Move mice into the microCT imaging chamber and place them onto the imaging box in the prone position, with noses facing perpendicular to nose cones. Use dental wax to gently restrain the feet on the imaging box to limit any movement. Up to 4 neonatal mice can be imaged at a time.

5.6 Turn the isoflurane vaporizer down to 2-4% flow to keep mice anesthetized during imaging. Shut the microCT imaging chamber door. Check on the mice a few seconds later. If they begin to move, douse a cotton ball in isoflurane and hold it to the nose of the animal moving for 5 seconds to anesthetize. Keep the cotton ball near the animals during imaging. Be careful not to over anesthetize and terminate the mice.

5.7 Using the software, choose the **Luminescent** option for imaging. Use an excitation filter set to **Block** and the emission filter set to **Open**, 500 nm, 520 nm, 560 nm, 580 nm, 600 nm, and 620 nm. There will be seven total emission filters set for luminescence.

5.8 Image the mice at each time point (0, 10, and 24 h post-infection [hpi]) and save all images to a folder for each time point. Return the pups to the cage with the dam and check that all pups have recovered from anesthesia.

5.9 To analyze 2D images, open images in the software. Change units to **Radiance (photons)**; this will turn into the **Total Flux (photons/second)**.

5.10 Only analyze one image set with its multiple emission filters at a time. From each image set, take note of the minimum and maximum radiance values located at the bottom right corner of each image (e.g., if there are 7 emission filters, there will be 7 images, and 7 minimum and maximum values). Repeat for each image set that is to be compared.

5.11 To determine a scale that will encompass the values and luminescence for all images, locate the lowest minimum value and the highest maximum value for each image set. For this study, the **Open** filter images were used as representative.

5.11.1. Highlight and open the image of choice to change the scale. On the **Tool Palette**, click on the **Image Adjust** tab and change the **Color Scale** to the lowest minimum and highest maximum

values previously identified. Save each image set as a TIFF. Individually analyze each time point in this manner to ensure the correct scale is displayed.

5.12 To quantify the total flux (amount of luminescent signal per mouse) for each individual mouse, open an image as previously described in step 5.9-5.10. Open the **ROI Tools** tab on the **Tool Palette** and select the circle tool. Choose **1** circle if analyzing one area of luminescence.

5.13 Move ROI to **Overlay** on the area of luminescence. Adjust the size of the ROI if necessary.

NOTE: If adjustment is necessary, adjust ROIs in other images comparably to maintain consistency. Choose **Measure ROIs**. The ROI Measurements window will open displaying **Total Flux (p/s)**, **Average Radiance (p/s/cm²/sr)**, **Standard Deviation of Radiance**, **Minimum Radiance**, and **Maximum Radiance**.

5.14 Record total flux measurements for each image set. This number is the quantified amount of luminescence in the mouse in 2D images.

5.15 To make 3D reconstructed microCT images, open the **DLIT 3D Reconstruction** panel on the **Tool Palette** and check all wavelengths to be included under the **Analyze** tab. Select **Reconstruct**.

6. Euthanasia

6.1 Prepare and label tubes for tissues/organs of interest for necropsy and appropriate downstream applications.

6.2 Separate the neonates from the dam in a biosafety cabinet.

6.3 Soak a cotton ball in veterinary-grade isoflurane and place inside of a transparent containment chamber.

6.4 If collecting blood, prepare a P200 micropipette with a tip and have a 1.5 mL tube with 10 μ L of 5 mM EDTA as an anticoagulant. A volume of 50-200 μ L of blood is expected.

6.5 Place a neonate in the chamber and monitor the pup until it becomes motionless.

6.6 Quickly, remove neonate and decapitate with scissors. If allowed to breathe fresh air for a prolonged period, the pup can regain consciousness. Neonates have reduced lung capacity relative to adult mice, and, therefore, do not breathe deeply enough for euthanasia by isoflurane alone.

6.7 Collect blood from the trunk at the base of the head using a P200 micropipette. To maximize the amount of blood collected, perform this step as quickly as possible following

decapitation. Enumerate bacteria in the blood by serial dilution and standard plate counting as described in step 1.9.

6.8 Sterilize the entire neonate with 70% ethanol prior to excision of tissue samples.

7. Tissue harvest

7.1 Within a biosafety cabinet, douse the neonate with 70% ethanol to prevent contamination. Lay the animal on its right side.

7.2 Using forceps, grasp the skin at a point between the abdomen and rear left leg and make an incision with fine-tipped surgical scissors. Continue to cut the skin away moving upwards towards the back. Progress until the entire spleen is exposed.

7.3 Use the forceps to grasp the spleen and remove it from the abdomen, using scissors to disconnect the connective tissue. Place the spleen in the solution appropriate for its downstream application.

7.4 To obtain the lungs, peel back the skin of the chest completely.

7.5 Entering at the base of the sternum with scissors held vertically, cut upwards until the rib cage is split.

7.6 Use forceps to grasp the right and left lungs individually and remove them from the thoracic cavity. Remove the heart from the lung tissue by cutting with scissors.

7.7 Place the lung in the solution appropriate for its downstream application. For RNA isolation, use 500 μ L of guanidine thiocyanate/phenol (GTCP). For histopathology, use 5 mL of 10% neutral-buffered formalin.

8. RNA isolation from lung tissue for gene expression

8.1 Pre-cool the microcentrifuge to 4 °C.

8.2 Mince the lung tissue in GTCP with scissors. Next, homogenize the tissue with a battery-powered homogenizer. Continue until the solution is as uniform as possible. Incubate at room temperature for 3-5 min.

8.3 Using filtered pipette tips, add 100 μ L of chloroform. Invert the tube for 15 s and incubate 3-5 min at room temperature.

8.4 Centrifuge for 15 min at 12,000 $\times g$.

8.5 During the spin, prepare 1.5 mL tubes with 500 μ L of 70% ethanol. Assemble and label the columns and collection tubes from the RNA isolation kit.

8.6 Carefully remove the top, aqueous layer without disturbing the interphase layer that formed during centrifugation. Place the aqueous layer in the tubes containing 70% ethanol.

8.7 Move the ethanol and lysate mixture to the column in the collection tube.

8.8 From this point on, follow the RNA isolation kit commercial product protocol until the final elution of RNA.

8.9 Analyze the RNA for purity and quantity. Use immediately or store at -80 °C until further use.

9. cDNA synthesis

9.1 Label PCR tubes and set aside.

9.2 Add 1 μ g of RNA to the cDNA reaction mixture for each sample.

9.3 Add the reagents and template to the PCR tube as described in the cDNA protocol. Add the enzyme to the mixture last.

9.4 Place PCR tubes in a thermocycler with the following run settings: 5 min at 25 °C, 40 min at 42 °C, 15 min at 85 °C and 4 °C final hold.

9.5 Remove PCR tubes from thermocycler and use immediately or store at -20 °C until further use.

10. Real-time quantitative PCR (qPCR) cycle

10.1 Prepare a reaction mix cocktail for each of the genes to be analyzed. Each 15 μ L PCR reaction requires 7.5 μ L of 2x reagent mix, 0.75 μ L of 20X 5'-FAM-labeled gene-specific primer/probe, and 3.75 μ L of nuclease-free water. Amplicons typically range from 60-120 bp.

10.2 Add 3 μ L of cDNA template for each experimental group to the appropriate wells.

10.3 Add 12 μ L of the gene-specific reaction mix cocktail to the appropriate wells.

10.4 Cover the plate with optical adhesive film and centrifuge for 1 min at 1,000 x g to remove any bubbles that may have formed in the wells.

10.5 Place the PCR plate in a real-time PCR thermocycler.

10.6 Set the run method as follows: 3 min at 95 °C, 40 cycles of 95 °C for 15 s followed by 60 °C for 1 min.

10.7 Analyze data by normalizing the gene of interest to an internal control and express data from infected samples relative to uninfected control samples using the 2^{-DDCt} formula and a \log_2 transformation of the numbers.

11. Lung histopathology

11.1 Remove the lungs from the neonatal pup as described above.

11.2 Place the tissue in a volume of 10% neutral-buffered formalin so that the ratio of solution to tissue is approximately 20:1 for 3-7 days.

11.3 Coordinate with an appropriate histology service for paraffin embedding, sectioning, and hematoxylin and eosin (H&E) staining. For this work, the West Virginia University Histopathology Core was utilized. Alternatively, follow previously described protocols¹⁹.

12. In vitro bacterial killing assay

12.1 Remove the spleen from the uninfected neonatal pup as described above and place it in a 40 μ m nylon basket within a sterile 60 mm Petri dish. Repeat this and pool spleens into one tube to be harvested and homogenized together.

12.2 Add 5 mL of PBS supplemented with 10% FBS.

12.3 Disaggregate the tissue using a sterile 3 mL syringe plunger until a single cell suspension is created.

12.4 Collect the single-cell suspension outside of the nylon basket, transfer to a 15 mL centrifuge tube, and pellet cells at 350 x g for 5 min.

12.5 Suspend the cells in red blood cell lysis buffer (2 mL for up to 7-8 spleens) and let it stand for 5 min at room temperature to eliminate erythrocytes.

12.6 Wash splenocytes with PBS and pellet as above.

12.7 Suspend the splenocytes in 0.25 mL of PBS supplemented with 0.5% BSA and 2 mM EDTA according to expected cell yield.

12.8 Count the splenocytes using a hemocytometer or other appropriate application.

12.9 Isolate Ly6B.2⁺ (myeloid population of granulocytes/inflammatory monocytes) cells with immunomagnetic beads according to manufacturer protocol.

12.10 Seed Ly6B.2⁺ cells at a density of 1×10^5 cells per well in a black or white 96-well plate in a volume of 0.1 mL of DMEM that contains 10% FBS, 2 mM glutamine, and 25 mM HEPES (complete medium).

12.11 Enumerate bioluminescent *E. coli* as described in section 1 and prepare the bacterial inoculum at the desired multiplicity of infection (MOI) in a final volume of 0.1 mL. This is best done by making what is necessary for all wells at a common MOI in batch.

12.12 Add 0.1 mL of bacterial inoculum or complete medium alone as a control. Incubate the multi-well plate at 37 °C and 5% CO₂ for 1 h.

12.13 Replace the media with 0.2 mL of fresh complete media that contains gentamicin (100 µg/mL) by gently removing media with a pipette and adding fresh media with a new pipette tip. Return the culture to incubation for an additional 2 h.

12.14 At 3 h post-infection, measure the luminescence in each well of the lidded culture plate from the bottom using a plate reader and then return the culture to incubation.

12.15 Repeat measurements of luminescence at other desired time points.

REPRESENTATIVE RESULTS:

This protocol induced bacterial sepsis in neonatal mice, and we used longitudinal intravital imaging, enumeration of bacteria in the blood, histological assessments of pathology, and inflammatory cytokine expression profiles to study the course of disease. Signs of morbidity were observed in neonatal pups infected with both low ($\sim 2 \times 10^6$ CFUs) and high ($\sim 7 \times 10^6$ CFUs) inoculums of *E. coli* over time. Pups that received the greater inoculum displayed more prominent signs of distress that included reduced mobility, the inability to correct their posture, and impaired ability to maintain an upright position by 24 h post-infection (hpi). There was, however, a range of morbidity as some pups appeared worse than others. Immediately following infection, one low-dose animal died due to isoflurane exposure during an imaging session to establish baseline. By 24 hpi, two of six high-dose animals succumbed to the systemic infection (33.3% mortality). Infected pups that received either a high or low dose inoculum weighed significantly less than their control littermates at 24 hpi (**Figure 1A,B**). All the pups that received the higher inoculum met endpoint criteria at 24 hpi. As such, all the infected pups in this group were euthanized following imaging. Bacteria in the blood were enumerated for a subset of mice that received the lower inoculum, and for all animals that received the higher inoculum since they were all euthanized. The results from two experiments performed similarly indicate that while most animals had high levels of bacteria in the blood (CFUs/mL) at 24 hpi, some animals did not have detectable bacteria in the blood (**Figure 1C**). The latter suggest that they cleared the infection by this time point. As expected, pups that received the higher inoculum had nearly three orders of magnitude more CFUs/mL at 24 hpi relative to pups that received the low dose inoculum (**Figure 1C**).

Live animal imaging of luminescent bacteria further confirmed the dissemination of bacteria and increase in growth in neonatal pups over time at 10 and 24 hpi (**Figure 2** and **Figure 3**). Additionally, using intravital imaging with the microCT, we were able to identify infection foci, including the brain (**Figure 2B**), lungs (**Figures 2B, 3A,B**), and other peripheral tissues (**Figure 2B**). The lungs of some highly infected mice demonstrated opaque regions consistent with inflammatory consolidation that co-localized to luminescent bacterial signal (**Figures 3A**). These regions of presumed inflammatory exudate are not found in uninfected control lungs (**Figure 3A**). Further evidence of a pronounced inflammatory cytokine response within the lungs of infected pups is demonstrated by gene expression analysis of IL-1 β , IL-6, and TNF- α . A significant increase in expression relative to controls was observed for all three cytokines in both the low and high inoculum groups (**Figure 4A**). Histopathology of the lung was also examined at 24 hpi in control and infected pups. Despite similar inflammatory cytokine profiles, a progressive increase in pathology was commonly observed from the lower to the higher inoculum. Compared with tissue from uninfected controls, the lungs of infected pups showed notable inflammatory changes, thickening of the alveolar wall, increased alveolar hemorrhaging, and inflammatory infiltration (**Figure 4B**). In the most severe infections, the pulmonary congestion and areas of hemorrhage contributed to a massive reduction in open air space (**Figure 4B**). Collectively, these results demonstrate that in our model of early onset neonatal sepsis, dissemination of luminescent bacteria can be followed over time from a subscapular inoculation site to important infection foci and cause significant inflammation and pathology in severely infected animals.

To study host factors that contribute to bacterial killing by innate immune cells such as monocytes, macrophages, and neutrophils, we developed a sensitive in vitro assay to measure bacterial clearance. Ly6B.2⁺ cells isolated from the spleens of neonatal mice were infected with bioluminescent *E. coli* at a range of MOIs for 1 h and then treated with gentamicin to kill extracellular bacteria. At 3, 6, 20, and 48 hpi, intracellular luminescence was measured with a multimode reader. As expected, with increasing MOI, more luminescent signal was recorded at 3 h (**Figure 5**). Gradually, this signal was lost, indicative of bacterial clearance (**Figure 5**). This assay is amenable to supplemented cytokines, neutralization of secreted effectors, and the addition of pharmacological inhibitors of cellular pathways to study interventions that may promote bacterial clearance and serve to improve outcomes in the neonatal sepsis model described here.

FIGURE AND TABLE LEGENDS:

Figure 1: Changes in body weight and bacterial replication in septic neonatal mice. (A,B)

Individual mouse weights within a group (low and high) expressed as a percentage of the mean weight of littermate control pups. Data are presented as mean percentage \pm SEM. Individual t-tests at each post-infection time point reveal significant differences at 24 h between control pups and pups that received the low inoculum ($p < 0.0001$) (**A**), or between control pups and pups that received the high inoculum ($p = 0.0031$) (**B**). (**C**) CFU/mL in the blood at 24 hpi were log transformed and presented as the mean \pm SEM. Mann-Whitney test reveals a trend towards significance between the low and high dose inoculums ($p = 0.0882$).

Figure 2: Intravital imaging demonstrates dissemination of bacteria in neonatal mice over time. (A) A representative neonatal mouse (#1) infected with an inoculum of $\sim 2 \times 10^6$ CFUs is shown at time 0, 10, and 24 hpi. A colorimetric scale with the minimum and maximum radiance values per time point are displayed for each time point. Mice at 0 and 10 h are displayed on both their time point scale and the 24 h scale to demonstrate changes in bacterial growth over time. **(B)** Representative 3D reconstructed microCT images of the same neonatal mouse at 10 and 24 hpi are shown. Each time point has images at overhead, transaxial, and coronal perspectives. In the transaxial image at 24 hpi, the plane has moved toward the periphery of the mouse to better display infection foci in the peripheral tissues. White arrows indicate the brain and kidney at 10 hpi and the kidney and lung at 24 hpi.

Figure 3: Lungs are a site of major infection during bacterial sepsis in neonates. (A) Representative 3D reconstructed microCT images of a neonatal mouse (#5) infected with an inoculum of $\sim 7 \times 10^6$ CFUs are shown at 24 hpi compared to an uninfected control. Both mice are displayed in the transaxial perspective and lungs are indicated by white arrows. The infected mouse was placed on two radiance (photons/sec) scales. Scale #1 includes all 6 wavelengths (500, 520, 560, 580, 600, 620 nm) and scale #2 includes only 500, 520, and 560 nm wavelengths. This second scale allowed to visualize an increased signal in bacteria in the lungs because lower wavelengths are more highly absorbed by tissue and produce stronger signal. **(B)** Representative 3D reconstructed microCT images of a neonatal mouse (#4) infected with an inoculum of $\sim 7 \times 10^6$ CFUs are shown at 24 hpi. This time point has images at the overhead, sagittal, transaxial, and coronal perspectives. White arrows indicate infection foci in the lungs.

Figure 4: Inflammation and associated histopathological findings in the lungs of septic neonates. At 24 hpi the lungs were harvested from pups that received $\sim 2 \times 10^6$ or 7×10^6 CFUs or uninfected controls. **(A)** RNA was isolated and the expression of IL-1 β , IL-6, or TNF- α as determined relative to uninfected controls by quantitative real-time PCR using the formula $2^{-\Delta\Delta C_t}$. The data is shown as the mean \log_2 transformed change in expression \pm SEM for each inoculum as indicated. Statistical significance was determined using unpaired t-tests of ΔC_t values between individual cytokine genes and the internal control in the 95% confidence interval. Asterisks indicate $p < 0.01$. **(B-D)** Histopathologic sections of H&E stained lung tissues (20x, area of interest constructed into clipping mask and enlarged for clarity) are shown. Lung tissues from a representative uninfected control **(B)** or infected neonate at the low **(C)** or high **(D)** inoculum are shown. Yellow arrows indicate alveolar thickening **(C)** or hemorrhaging **(D)**. Scale bar = 500 μ m.

Figure 5: An in vitro assay for bacterial clearance. Ly6B.2⁺ cells were isolated from the spleens of uninfected control neonates. Cells were seeded in 96-well plates and infected with luciferase-expressing *E. coli* O1:K1:H7 at a multiplicity of infection (MOI) of 10, 50, or 250 as indicated. After 1 h, the medium was replaced with fresh that contained gentamicin (100 μ g/mL). Mean relative light units (RLU) \pm SE for an individual experiment representative of multiple are shown. Statistical significance in the 95% confidence interval was determined using unpaired t tests with Welch's correction; asterisks indicate $p < 0.05$.

DISCUSSION:

Our subscapular infection model for inducing bacterial sepsis in neonatal mice is a novel method to study the longitudinal spread of bacterial pathogens in real time. Intravital imaging provides the opportunity to explore bacterial dissemination in real time in neonates. This is critical to understand the kinetics of bacterial dissemination and to further study the host response and damage at the appropriate phase of disease. Mouse pups are administered a subcutaneous, subscapular injection of bacterial inoculum. This injection technique is simpler than other commonly used alternatives, such as the tail vein and intraperitoneal infections, as it requires less precision within an injection site. This is important given the small size of the pups. The intravital imaging allows for a longitudinal assessment of bacterial proliferation and dissemination into peripheral tissues and the central nervous system over time without the need to sacrifice the animal. Similar imaging approaches and technologies have been used for the study of cancer biology and metastasis^{20,21}. Furthermore, while another study has cited the use of bioluminescent imaging during an *E. coli* infection in neonatal rats²², here, we have applied the approach to neonatal mice, wherein our methodology allows evaluation of bacterial kinetics during murine sepsis. Visualization of the bacteria is based on emission of bioluminescent light at various wavelengths from bacteria (e.g., bacterial luciferase activity) within the animal. Bioluminescence is then visualized through a cooled charged coupled device (CCD) camera. The resulting visualized bioluminescence can then be reconstructed into a 3D image that shows both spatial- and temporal-dependent effects of bacteria within an animal. For an added, more nuanced layer of data acquisition, successful animal identification through tail tattoo allows for a repeated measures assessment of individual pups across time and the identification of possible outliers within a given experimental group.

The most successful application of the described model requires accuracy in preparation of the bacterial inoculum. Here, we describe an optimized method for bacterial preparation using a pre-established and validated *E. coli* growth curve that reduces variation between the target and actual inoculum. This allows experimental reproducibility at an intended inoculum. The inclusion of two inoculums in our model demonstrated dose-dependent outcomes in blood CFUs, mortality, and lung pathology. However, some aspects of the disease trajectory were not dose dependent. The failure to gain weight in infected animals was not dependent on the inoculum at 24 hpi. Additionally, similar levels of inflammatory cytokine expression were observed in the lung in response to infection with both inoculums. Whether or not this pattern would be replicated in all tissues where bacteria were observed, such as the kidney, liver, spleen and brain, remains to be determined. In addition to sepsis, *E. coli* O1:K1:H7 is associated with meningitis in the neonatal population²³. This brain infection occurs when bacteria from the periphery invade and penetrate the blood brain barrier. Future studies will explore this aspect of the model through analysis of changes in tight junction protein expression, as well as test different ranges of bacterial inoculums. An additional modification during intravital imaging includes the addition of a singular cotton ball, doused in isoflurane, which is placed approximately 2-3 inches away from the mice during imaging. In response to previous experiments wherein the neonatal pups have regained consciousness during the imaging session, preventing accurate image acquisition, we now place the cotton ball close enough to

the mice to keep them continuously anesthetized during imaging. However, it is important this is not done so close that they fail to recover from the anesthesia.

Although flexible and easily adaptable for the study of the kinetics of different bacteria in various animal and disease models, our protocol has some limitations to consider. The first limitation to consider is that the subscapular route of infection does not mirror a natural route of transmission. However, a primary objective in the development of our model from the outset was to establish an easily reproducible mode of delivery that could be used to establish a systemic infection that replicates aspects of human disease. Therefore, in this report, we describe a model of human early onset sepsis disease syndrome, not a model of natural transmission. There is an established model of oral delivery in neonatal rats that replicates some aspects of common human transmission, such as initial colonization of *E. coli* infection in the alimentary canal and subsequent dissemination to the bloodstream and peripheral tissues, including the brain²². The model established by Witcomb and colleagues also incorporates bioluminescent *E. coli* and intravital imaging. Moreover, it is crucial to minimize isoflurane exposure, as well as inject, tail tattoo, and handle pups as quickly as possible without compromising accuracy and precision of the techniques in an attempt to mitigate stress levels for both the neonates and the dams. In some cases, if the pups experience enhanced human-induced and/or experimental manipulations, the dams can stop nursing and caring for the pups, resulting in decreased survival unrelated to the infection. Similarly, pups that are exposed to isoflurane for prolonged periods beyond the approximate 10 minutes of an imaging session have an increased risk of death; thus it is crucial to supply just enough isoflurane to sufficiently anesthetize the mice, but not enough to euthanize them. A final point of consideration is the limit of sensitivity. Tissues in which less than 10^4 CFUs/mL *E. coli* were enumerated the luminescent signal recorded falls at the low end of the detectable range, according to the scaling method used in the imaging software³. Thus, some tissues may be colonized with low levels of bacteria but appear without visible bioluminescence.

Currently, most studies utilize adult methods of bacterial dissemination, such as intraperitoneal (i.p.) and tail vein injections for neonates. Pluschke and Plekonen analyzed the effect of *E. coli* K1 on neonatal mice through i.p., tail vein, and oral infections²⁴. This study demonstrated that different genotypes of mice with immunodeficiencies are more susceptible to the K1 strain; however, many aspects of host immune response to infection as well as the mechanisms for bacterial spread are left unaddressed. Deshmukh and colleagues infected neonatal mice intraperitoneally with *E. coli* K1 or *K. pneumoniae* and measured CFUs in the spleen and liver at 72 hpi²⁵. This study also analyzed some aspects of host response to infection based on pre-exposure of mice to antibiotics. However, thorough investigation of bacterial dissemination to peripheral tissues and blood over time in parallel with inflammatory profiling in the same tissue (other than granulocytosis) was not addressed. Other studies of neonatal sepsis in mice with *Staphylococcus aureus*, *Staphylococcus epidermidis*, Group B *Streptococcus*, and *E. coli* explore varying aspects of the host immune system in response to infection. However, none of these studies utilize intravital imaging to explore the kinetics of bacterial dissemination or localization of infection foci²³⁻²⁶. Our method of infection and intravital imaging, combined with bacterial burden assessment and inflammatory profiling of peripheral tissues, allows us to

comprehensively examine aspects of both the host and pathogen during infection, providing a more precise understanding of host-pathogen interplay during sepsis.

We intend to utilize this infection and imaging model to further our understanding of early-onset neonatal sepsis using a variety of pathogenic bacteria commonly responsible for sepsis in neonates, including Group B streptococci, *K. pneumoniae*, and *Listeria monocytogenes*. This infection model will allow us to longitudinally compare dissemination of different bacterial pathogens in parallel with the host response in neonates. In addition, this model is adaptable to the adoptive transfer of specific (fluorescently conjugated) immune cell types to study their migration to sites of infection and subsequent influence on the host response and control of bacteria. This grants the opportunity to better understand the host-pathogen interactions that occur during sepsis in early life in ways that have not been previously demonstrated.

ACKNOWLEDGMENTS:

This work was supported by institutional funds to C.M.R.

DISCLOSURES:

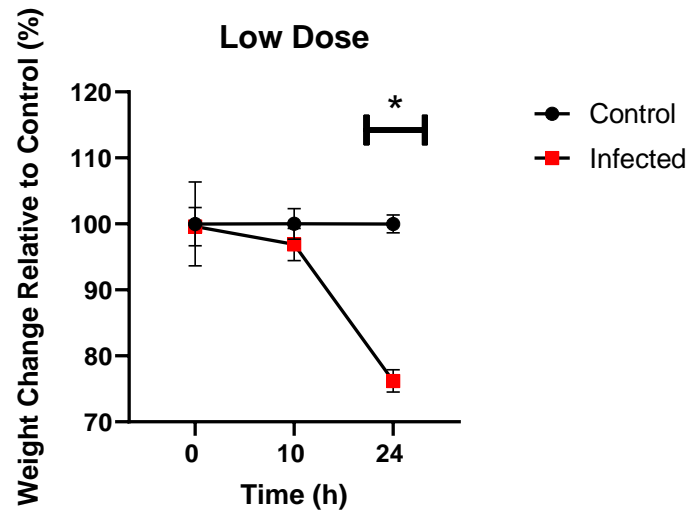
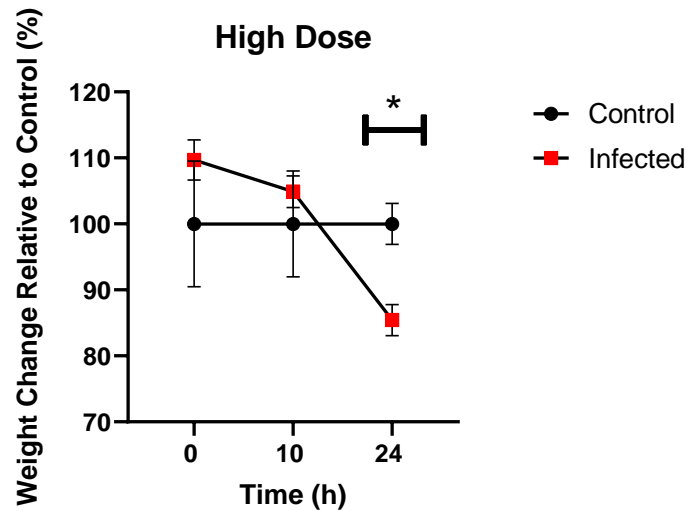
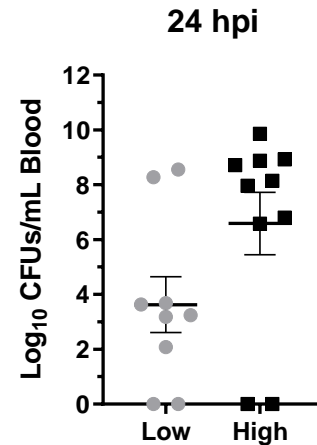
The authors have no conflicts of interest to disclose.

REFERENCES:

1. Qazi, S. A., Stoll, B. J. Neonatal sepsis: a major global public health challenge. *Pediatr Infect Dis J.* **28** (1 Suppl), S1-2 (2009).
2. Simonsen, K. A., Anderson-Berry, A. L., Delair, S. F., Davies, H. D. Early-onset neonatal sepsis. *Clinical Microbiology Reviews.* **27** (1), 21-47 (2014).
3. Seman, B. G. et al. Elevated levels of interleukin-27 in early life compromise protective immunity in a mouse model of Gram-negative neonatal sepsis. *Infections and Immunity.* (2019).
4. Schrag, S. J. et al. Epidemiology of Invasive Early-Onset Neonatal Sepsis, 2005 to 2014. *Pediatrics.* **138** (6), e20162013 (2016).
5. Stoll, B. J. et al. Early onset neonatal sepsis: the burden of group B Streptococcal and E. coli disease continues. *Pediatrics.* **127** (5), 817-826 (2011).
6. Weston, E. J. et al. The burden of invasive early-onset neonatal sepsis in the United States, 2005-2008. *Pediatrics and Infectious Disease Journal.* **30** (11), 937-941 (2011).
7. Hornik, C. P. et al. Early and late onset sepsis in very-low-birth-weight infants from a large group of neonatal intensive care units. *Early Human Development.* **88 Suppl 2** S69-S674 (2012).
8. Vergnano, S., Sharland, M., Kazembe, P., Mwansambo, C., Heath, P. T. Neonatal sepsis: an international perspective. *Archives of Disease in Childhood: Fetal and Neonatal Edition.* **90** (3), F220-224 (2005).
9. Kraft, J. D. et al. Neonatal macrophages express elevated levels of interleukin-27 that oppose immune responses. *Immunology.* **139** (4), 484-493 (2013).
10. Basha, S., Surendran, N., Pichichero, M. Immune responses in neonates. *Expert Reviews of Clinical Immunology.* **10** (9), 1171-1184 (2014).

11. Gleave Parson, M. et al. Murine myeloid-derived suppressor cells are a source of elevated levels of interleukin-27 in early life and compromise control of bacterial infection. *Immunology and Cell Biology*. **97** (5), 445-446 (2018).
12. Adkins, B., Leclerc, C., Marshall-Clarke, S. Neonatal adaptive immunity comes of age. *Nature Reviews Immunology*. **4** (7) 553-564 (2004).
13. Kim, S. K., Keeney, S. E., Alpard, S. K., Schmalstieg, F. C. Comparison of L-selectin and CD11b on neutrophils of adults and neonates during the first month of life. *Pediatrics Research*. **53** (1), 132-136 (2003).
14. Velilla, P. A., Rugeles, M. T., Chougnet, C. A. Defective antigen-presenting cell function in human neonates. *Clinical Immunology*. **121** (3), 251-259 (2006).
15. Le Garff-Tavernier, M. et al. Human NK cells display major phenotypic and functional changes over the life span. *Aging Cell*. **9** (4), 527-535 (2010).
16. Weinberger, B. et al. Mechanisms underlying reduced responsiveness of neonatal neutrophils to distinct chemoattractants. *Journal of Leukocyte Biology*. **70** (6), 969-976 (2001).
17. Gabrilovich, D. I., Nagaraj, S. Myeloid-derived suppressor cells as regulators of the immune system. *Nature Reviewss Immunology*. **9** (3), 162-174 (2009).
18. National Research Council. 2011. *Guide for the care and use of laboratory animals*, 8th ed. National Academies Press, Washington, DC.
19. Tucker, D. K., Foley, J. F., Bouknight, S. A., Fenton, S. E. Sectioning Mammary Gland Whole Mounts for Lesion Identification. *Journal of Visualized Experiments*. (125), e55796, (2017).
20. Bayarmagnai, B., Perrin, L., Esmaeili Pourfarhangi, K., Gligorijevic, B. Intravital Imaging of Tumor Cell Motility in the Tumor Microenvironment Context. *Methods in Molecular Biology*. **1749**, 175-193 (2018).
21. Beerling, E., Ritsma, L., Vrisekoop, N., Derksen, P. W., van Rheenen, J. Intravital microscopy: new insights into metastasis of tumors. *Journal of Cell Science*. **124** (Pt 3), 299-310 (2011).
22. Witcomb, L. A., Collins, J. W., McCarthy, A. J., Frankel, G., Taylor, P. W. Bioluminescent Imaging Reveals Novel Patterns of Colonization and Invasion in Systemic Escherichia coli K1 Experimental Infection in the Neonatal Rat. *Infection and Immunity*. **83** (12), 4528 (2015).
23. Singh, K. et al. Inter-alpha inhibitor protein administration improves survival from neonatal sepsis in mice. *Pediatric Research*. **68** (3), 242-247 (2010).
24. Mancuso, G. et al. Role of interleukin 12 in experimental neonatal sepsis caused by group B streptococci. *Infections and Immunity*. **65** (9), 3731-3735 (1997).
25. Thammavongsa, V., Rauch, S., Kim, H. K., Missiakas, D. M., Schneewind, O. Protein A-neutralizing monoclonal antibody protects neonatal mice against Staphylococcus aureus. *Vaccine*. **33** (4), 523-526 (2015).
26. Andrade, E. B. et al. TLR2-induced IL-10 production impairs neutrophil recruitment to infected tissues during neonatal bacterial sepsis. *Journal of Immunology*. **191** (9), 4759-4768 (2013).

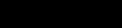
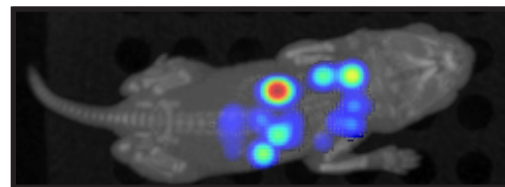
Figure 1

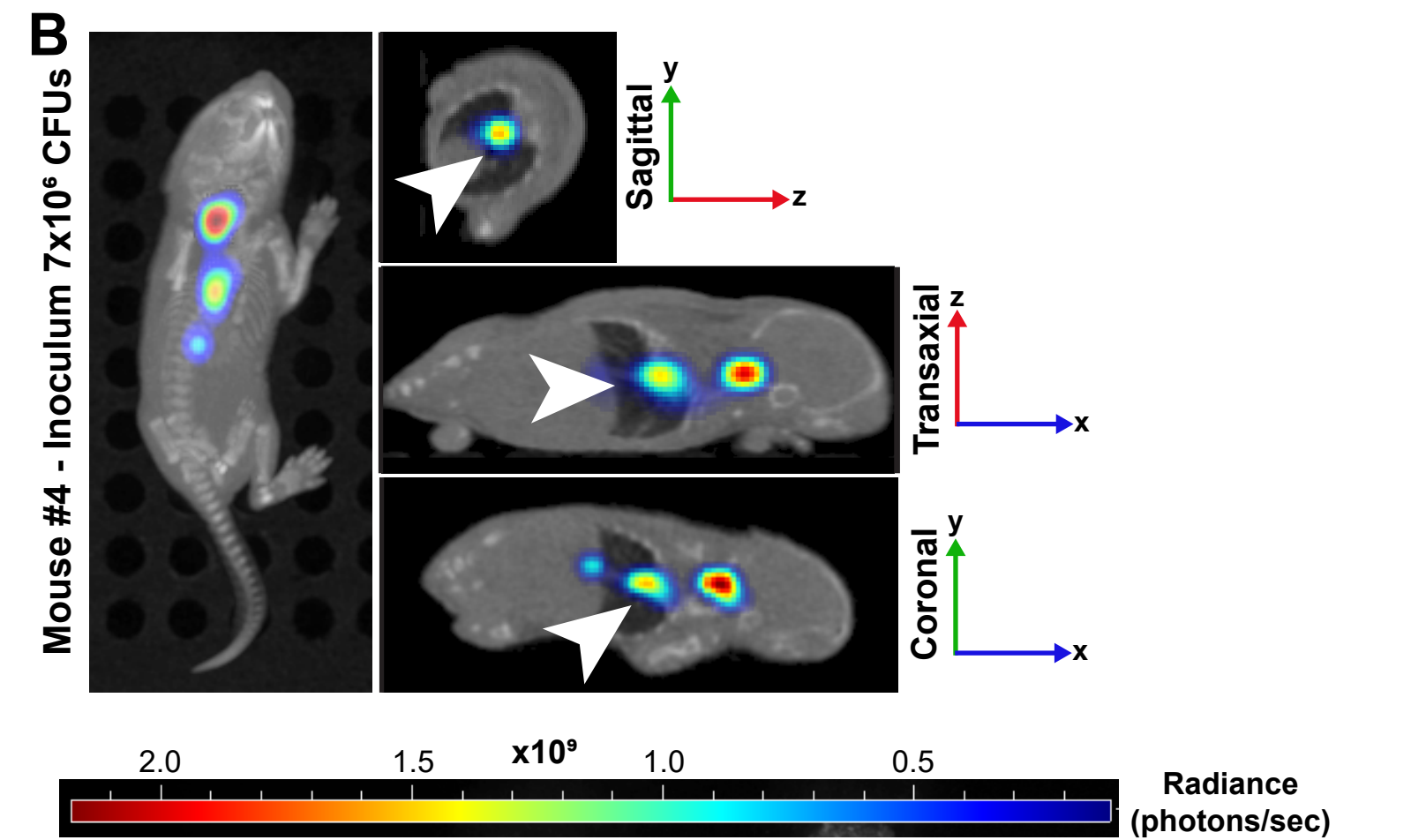
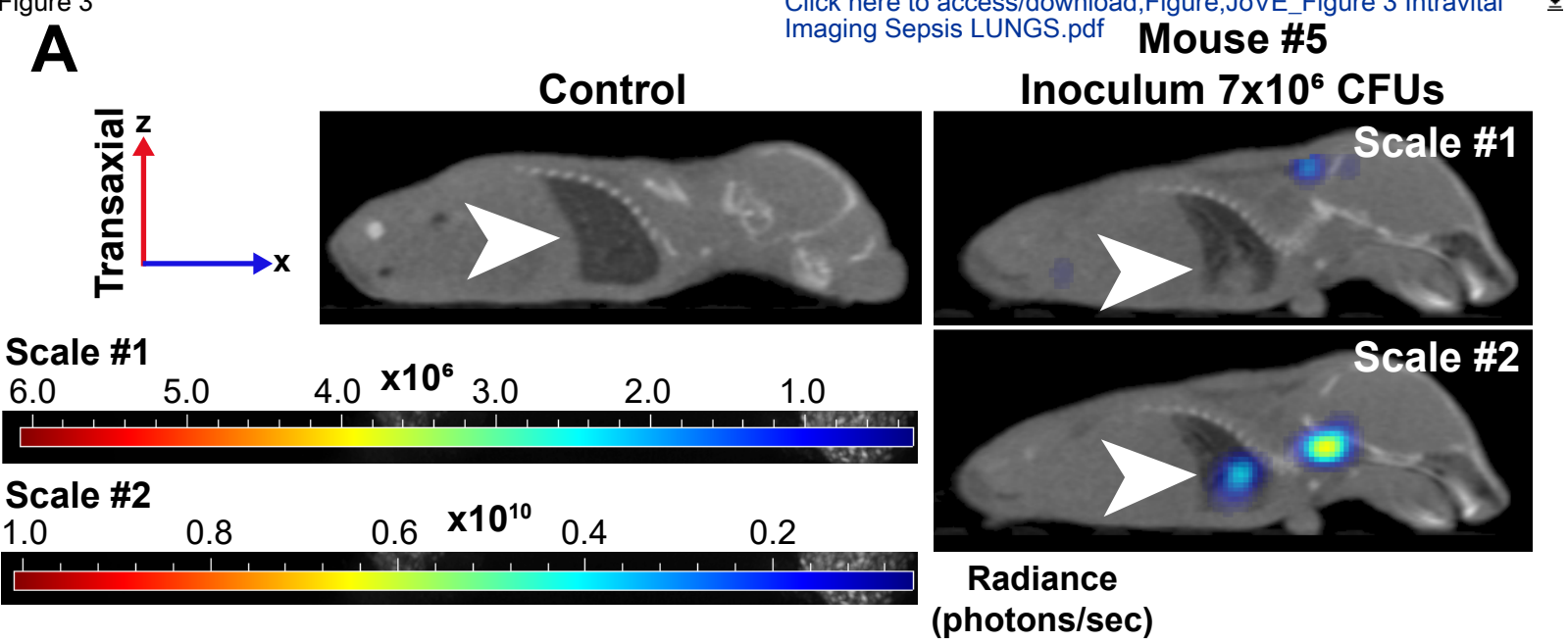
[Click here to access/download;Figure;JoVE_Figure 1_Weights and Blood CFUs.pdf](#)**A****B****C**

A



24 hpi





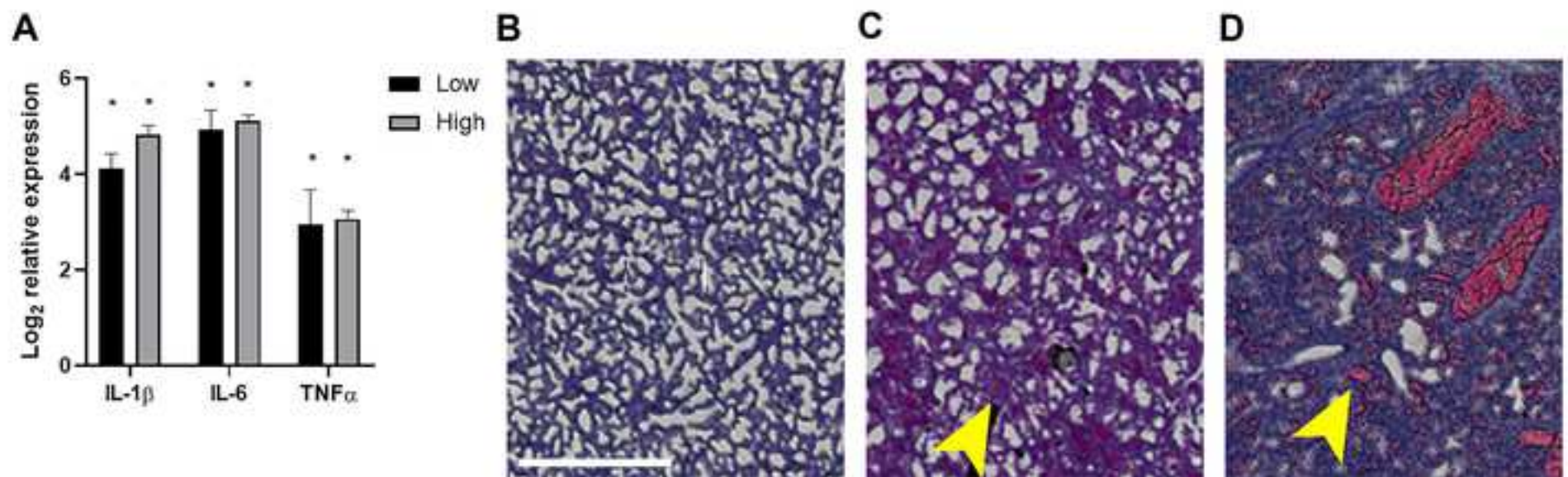
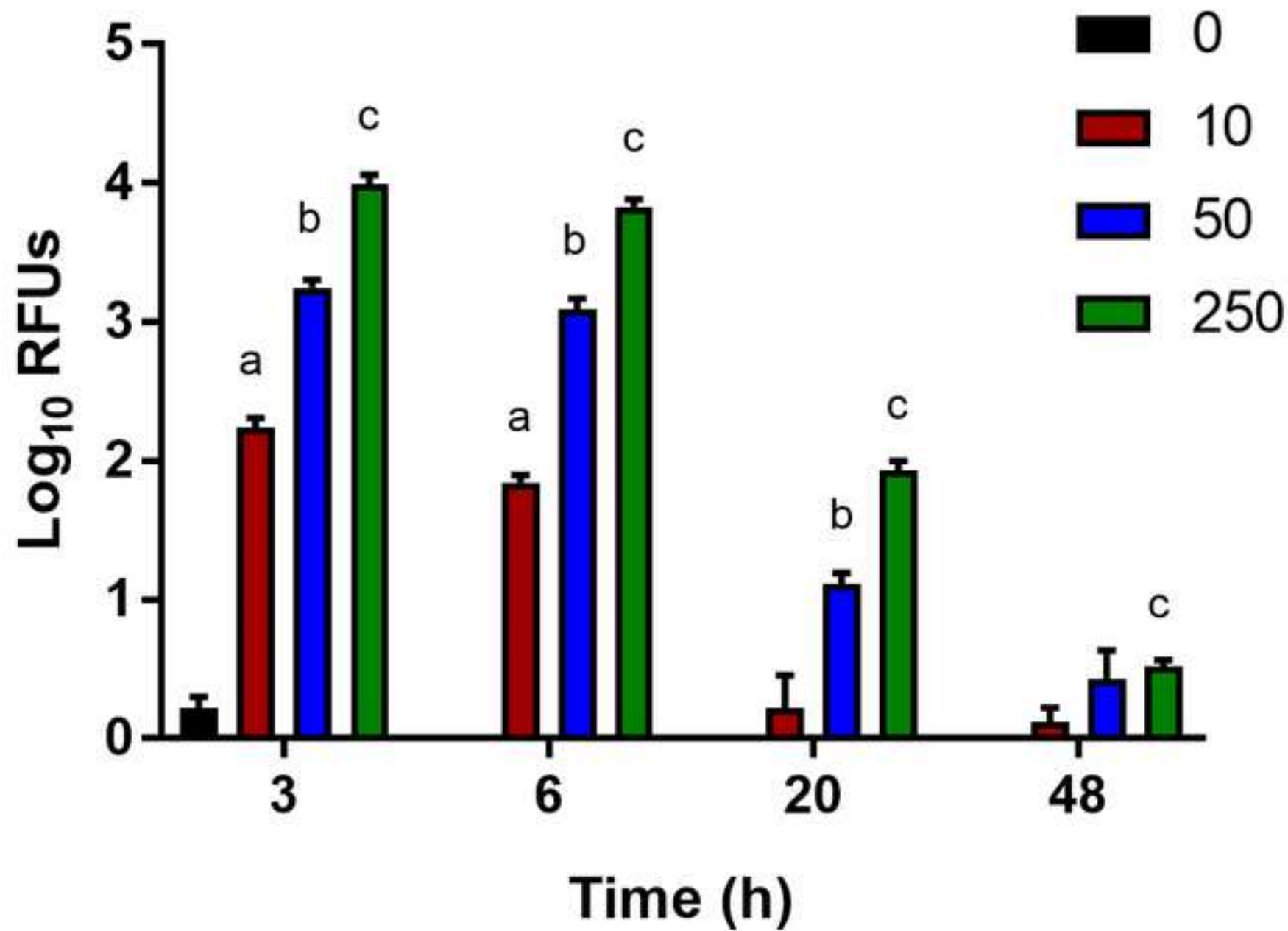


Figure 5



| Name of Material/ Equipment | Company | Catalog Number | Comments/Description |
|---|-------------------------------|----------------|-----------------------------|
| 1 mL Insulin Syringe | Coviden | 1188128012 | Inoculum or PBS injection |
| 10% Neutral Buffered Formalin | VWR | 89370-094 | Histopathology |
| ACK Lysis Buffer | Gibco | LSA1049201 | Bacterial clearance assay |
| Animal Tattoo Ink Paste | Ketchum | KI1482039 | Animal identification |
| Animal Tattoo Ink Green Paste | Ketchum | KI1471039 | Animal identification |
| Anti-Ly-6B.2 Microbeads | Miltenyi Biotec | 130-100-781 | Cell isolation |
| <i>Escherichia coli</i> O1:K1:H7 | ATCC | 11775 | |
| <i>Escherichia coli</i> O1:K1:H7- <i>lux</i> (expresses luciferase) | N/A | N/A | Constructed in-house at WVU |
| E.Z.N.A. HP Total Extraction RNA Kit | Omega Bio-tek | R6812 | RNA extration |
| DPBS, 1X | Corning | 21-031-CV | |
| Difco Tryptic Soy Agar | Becton, Dickinson and Company | 236950 | Bacterial growth |
| IL-1 beta Primer/Probe (Mm00434228) | Thermo Fisher Scientific | 4331182 | Cytokine expression qPCR |
| IL-6 Primer/Probe (Mm00446190) | Thermo Fisher Scientific | 4331182 | Cytokine expression qPCR |
| iQ Supermix | Bio-Rad | 1708860 | Real-time quantitative PCR |
| iScript cDNA Synthesis Kit | Bio-Rad | 1708891 | cDNA synthesis |
| Isolation Buffer | Miltenyi Biotec | N/A | Bacterial clearance assay |
| IVIS Spectrum CT and Living Image 4.5 Software | Perkin Elmer | N/A | Intravital imaging |
| LB Broth, Lennox | Fisher BioReagents | BP1427-500 | Bacterial growth |
| EASYstrainer (Nylon Basket) | Greiner Bio-one | 542 040 | Cell strainer |
| SpectraMax iD3 | Molecular Devices | N/A | Plate reader |
| Pellet Pestle Motor | Grainger | 6HAZ6 | Tissue homogenization |
| Polypropylene Pellet Pestles | Grainger | 6HAY5 | Tissue homogenization |
| Prime Thermal Cycler | Techne | 3PRIMEBASE/02 | cDNA synthesis |
| TNF-alpha Primer/Probe (Mm00443258) | Thermo Fisher Scientific | 4331182 | Cytokine expression qPCR |
| TriReagent (GTCP) | Molecular Research Center | TR 118 | RNA extration |



July 6, 2020

Dear Dr. Bajaj:

Thank you for the review of our manuscript and the opportunity to submit a revised version of our previous submission (JoVE61609). All of the editorial comments were considered and addressed. The exception is for item 11 regarding permission to use a figure from a previous publication as this is not applicable. For simplicity sake, we did not list these since they were uniformly acknowledged without need for additional response. We have also carefully evaluated the reviewers' concerns and comments and have addressed these below. Our responses follow reviewer comments in red font. Changes to the text in the manuscript have been highlighted. We look forward to your reply regarding our revision.

Sincerely,

A handwritten signature in black ink that reads 'Cory Robinson'.

Cory Robinson

Reviewers' comments:

Reviewer #1:

Manuscript Summary: This method paper was very well written and mostly clear throughout. My suggestions below might help to clarify points for the reader but overall this is a good model for the neonatal sepsis field.

Major Concerns:

While this is not a 'major concern' the manuscript needs to contain further information about: Statement of ethics i.e. permissions required for the animal work.

This was added following the Discussion.

Methods Step 3. How many pups are used per experiment/treatment/timepoint? How are pups randomised - e.g. same litter has mix of control and infected pups, or are different litters treated separately. Are litters synchronised (e.g. using Whitten effect) or are dams checked for fertilisation and there are enough matings set up to anticipate sufficient litters together. How much variability in pup age is acceptable? What is the age limit of the infection model. Does pup skin colour have any effect, and at what age does hair start growing and does this impact imaging quality.

The total number of pups used per experiment, treatment (control, low dose, or high dose), and timepoint (0, 10, and 24 hours) has been included in section 3.1. As well, it has been clarified that each litter received its own treatment (i.e., one litter is designated to receive the high dose inoculum, and another, separate litter that is age-matched within a day is designated to receive the low dose inoculum. Within each litter, 2-4 mice were used as controls. For this work, timed-pregnant females were purchased from Jackson Laboratories. As mentioned in the third paragraph of the introduction in the manuscript, in this model the pups are infected on postnatal day 3 or 4. This detail was also added to section 3.2. Pup skin color does not impact imaging quality, nor does the growth of hair, although the latter is not relevant in the first 2 days of infection reported here, as C57BL/6 neonates do not begin to grow hair until approximately postnatal day 6.

Abstract - the authors should not include a 10^4 cfu limit on detection in the abstract if they do not demonstrate this in the methods. This would have been a helpful addition and would help to clarify the limitations of the model. Since this appears again in the discussion (line 535) the authors should include this data unless it is already published elsewhere.

The reference to a CFU limit has been removed from the abstract. The text in the Discussion has been modified and previous related work cited. Although a formal experiment to discern a strict limit of detection has not been performed, a range of bacteria in specific tissues and corresponding luminescent signal has been reported and can be used for an understanding of relative sensitivity.

Minor Concerns:

Title - add in 'imaging'

This was added as requested.

The following points are numbered according to the steps in the Methods.

Steps 1.7 and 1.8 are currently written in quite an unclear way to understand the protocol. 1.7 should start with the target dose specified - i.e. that each mouse will receive inoculums of 2×10^6 or 7×10^6 , and then direct the reader to the calculation method. It should also state that the reader might need plenty of extra for the injections. It would not be a good idea to only prepare sufficient for the specific number of pups to be injected.

Bulleted steps along with an equation were added to step 1.7 to enhance clarity.

1.8. This should state that bacteria should be resuspended so that inoculum is in 50 μ l dose per mouse. i.e. if preparing 10 doses at 2×10^6 per inoculum, then 2×10^7 bacteria should be suspended in 500 μ l PBS. And again make the suggestion that the reader would need plenty of excess to enable sufficient for preparation of injections. What is pH of PBS used (and recipe?)

Additional text was added to enhance clarity. The pH for PBS was also added.

3. Can the authors comment on alternative infection routes and why they chose this one?

As mentioned in the third paragraph of the Introduction in the manuscript, there are technical difficulties surrounding alternative infection routes (i.e., tail vein, oral gavage, or intraperitoneal injections), and thus why subscapular injection was selected. Our method offers an ease of inoculation that results in a systemic infection that models aspects of human neonatal sepsis. We have also added brief text to section 3.6 of the methods.

4.6 - 'steps 4-6' Do the authors mean steps 4.4-4.6? Are pups euthanised if they reach any, or all, of the criteria? Authors use a 24 h timepoint as an endpoint in some experiments, can they expand on timepoint decisions. Authors should note at what timepoint control pups are also killed. They touch on this in the results section (line 390) but it would be helpful to flag up in the methods section.

The numbering has been corrected in the revised manuscript.

Pups are euthanized once they meet any of the endpoint criteria (which are now bulleted under step 4.4). The 24 h time point is a critical period for pups that receive either inoculum and peak disease is often observed. Pups that receive the high dose frequently meet endpoint criteria before 48 h post-infection. Control pups are also euthanized at this time point to allow for comparative analysis between the two experimental groups (control vs infected).

5.4 - this stage should be at 5.2, before the neonates are anesthetized, to allow stage to heat to 37°C.

This change was made as requested.

5.7 - Can the authors expand on the reason for choosing multiple emission filters - is this specific to the 3D microCT reconstruction and is there an optimal setting for the bioluminescence. It would be helpful for the authors to also give more settings here, e.g. do they use varying exposure times, binning preference, etc.

In general, firefly luciferase has a broad emission spectrum which ranges from 500 to 700 nm, which is why we choose to use so many emission filters so that we can get as much signal from throughout the mouse as possible. Exposure times are chosen by the imaging software during imaging and is based on how strong the signal is from the mice. Binning is also chosen by the software.

6.4 - it would be helpful to suggest size of pipette that might be needed. E.g. a P200 Gilson? How much blood do they expect to collect by this route.

We use a universal P200 pipette tip. It is likely to expect a volume of 50-200 µL of blood per animal. This has been added to the text in the manuscript in section 6.4.

7. Do the authors image the excised organs to get a specific bioluminescence measure of tissue distribution prior to downstream applications? This is a useful way to demonstrate that bioluminescence originates in a specific organ.

We have not imaged the excised organs directly, but this is a useful suggestion to incorporate into future studies. However, it is possible that the tissue could dry significantly during the approximate 10 min required to image and thus influence downstream applications. This would need to be carefully evaluated. Alternatively, harvested tissues could be placed in wells of a multi-well dish with equivalent amounts of PBS and bioluminescence quantified with a multi-mode reader or luminometer.

9.2 Authors should state use of BioRad iScript cDNA Synthesis Kit

The authors have removed the use of the BioRad iScript Synthesis Kit from the manuscript text (as with all other references to commercial items), but have included it in the Table of Materials.

10.1 - it might be useful to have a little more information on the authors' approach to qPCR, e.g. a quick introduction on what size fragments the authors generally aim for, or refer to prior publications for the same cytokine expression to direct the reader to more in depth methodology. The PCR recipe needs appropriate concentration of primer/probe. Do the authors use SYBR green or Taqman approach i.e. DNA dye or fluorogenic probe, and any particular reason for this.

We have provided the concentrations of all qPCR reaction components in section 10.1. As well, we have included primer information in the Table of Materials. Amplicons in these assays typically range from 60-120 bp in length. We prefer Taqman assays over SYBR green incorporation because it minimizes signal from non-specific amplicons and/or primer hybridization. However, this is only our laboratory preference and we do not consider ourselves experts on PCR chemistry. For this reason, we have not provided a recommendation for one chemistry over another.

12.1 'Pool each spleen' - do the authors collect all the spleens from different animals together? Is this just spleens from uninfected animals (before addition of further bioluminescent *E. coli* in 12.11). Or are there no spleen-localised *E. coli* in the infected animals?

For isolation of cells for in vitro assays, the spleens from uninfected animals are pooled. Bacteria are not added to the cultured cells until step 12.1.

How many experimental repeats do they recommend.

We recommend 3 independent experimental replicates to demonstrate reproducibility for most reported observations. However, this could vary and require additional replicates depending on the experimental details. We have established an in vitro assay that can be used for a variety of questions and is amenable to cytokine neutralizations, pharmacologic inhibitors of cellular pathways, other interventions, etc.

12.9 - what cell type is isolated by Ly6B.2+ extraction.

Ly6B.2⁺ cells are a population of myeloid cells that include neutrophils and inflammatory monocytes.

12.10 - how long after seeding cells should the killing assay be performed. Is there a time limit on the viability of the Ly6B.2+ cell culture? Are there any stages at which the experiment can be paused - e.g. whole spleen in the fridge, splenocytes frozen (details of freezing media and for how long), etc.

The Ly6B.2⁺ cells can be infected immediately after seeding. We have not empirically determined a time period at which the cells can be cultured resting before infection. Since neutrophils are present in this cell population and do not have extended viability, a significant waiting period is not recommended. We have not measured the viability of Ly6B.2⁺ cells over time. This can be done at reviewer request, but we will need sufficient time to generate a new litter of neonates, age them to at least 4 days, isolate cells, and perform the viability assay. Spleens should not be stored chilled or frozen for later primary cell isolation. This would result in significant loss of viability and selection of certain mononuclear populations that would better survive the freeze-thaw process. It is also not clear what effect this would have on cellular activity and phagocyte function.

12.12 should read 0.1 mL

This change has been made.

Lines 385-396. It would be helpful to know how many animals are referred to e.g. 2 high-dose animals succumbed to the infection within 24 hpi - what percentage of the group is this?

In this report, 2 of 6 mice that received the high dose were not viable at 24 h, so this is equivalent to 33.3% of this group. This percentage has been added to the text.

Fig 2 - this would be an ideal point to demonstrate how the different scales can be changed to accommodate all the images. At present the color scale is set to max/min for each individual image. If the color scales of the earlier time points were adjusted so that their scale matched the 24 hpi timepoint, then it would be clear how much more bacterial luminescence there is at this later time.

We have included images both ways. Panel A shows the same mouse over time on a common scale and as was previously submitted. It is clear that this mouse has an increase in bioluminescence by 24 h compared to earlier time points (the scale increases >2-fold), but we agree with the reviewer that a common scale simplifies the interpretation. We also think that including the images as presented previously is also important to emphasize the total bioluminescence at each time point.

Fig 3 - can the authors explain a little more what the difference in the wavelengths means, and how this changes the visible bioluminescence signals in the same mouse i.e. scale 1 has two bioluminescent spots in the head and neck region, while scale 2 has 2 different spots in lung and throat(?).

Absorption of photons in the far-red spectrum in mammalian tissues is low (this is 600-700 and beyond nm), though absorption is higher in the blue/green spectrum (500s nm). In these images, we chose to show emission filters from the blue/green spectrum (scale 2) which will give us higher absorption and will therefore provide a stronger signal (Kuo C, 2007, J. Biomed. Optics). This signal is utilized to show the localization of bacteria that is found within the lung and thymus regions of the mouse. In particular for panel A, when we use scale 1 (including all of the emission filters), a weaker signal is generated. This allows us to show the CT portion of the lung without the bacterial signal, and highlight the opaque region indicative of consolidation that colocalizes with bacteria observed with scale 2. The opaque region analogous to what is observed on chest film is not observed in control pups. This is an important feature to highlight since we focus on lung inflammation and pathology in Figure 4.

Given that *E. coli* O1:K1:H7 is associated with meningitis as well as sepsis, the authors should mention brain infection and how this might be investigated at some point in the manuscript (e.g. in section 7 or in discussion), even if they do not go into method detail.

We have briefly discussed the association between *E. coli* O1:K1:H7 and meningitis in the discussion, paragraph 2, and how we might investigate the effects of this strain of bacteria on the brain. This is an active area of research in our laboratory.

Table of materials needs a few additions: tattoo ink, tryptic soy agar and LB - are both of these purchased, if so, state where from. If not, give recipe. Ditto PBS, neutral-buffered saline, neutral-buffered formalin.

These have been added as requested.

One reference that should probably be included is Witcomb et al (2015) Infect. Immun. 83:4528-4540 Bioluminescent imaging reveals novel patterns of colonization and invasion in systemic *Escherichia coli* K1 experimental infection in the neonatal rat.

We have included text that describes this publication in the Discussion. We thank the reviewer for alerting us to important literature that was not included.

Reviewer #2:

Manuscript Summary: This protocol thoroughly lays out methodology for a model of late-onset neonatal bacterial sepsis. It includes how to infect pups, monitor the infection during the course, and several protocols for endpoint assessment of infection.

Major Concerns:

While this is a very detailed protocol that includes an in depth discussion of the context of bacterial

infections in prematurely born populations, the authors should include a discussion of the limitations of this model. Notably, how does the subcapsular injection reflect the route of infection in clinical sepsis cases, particularly given the fact the authors are using *E. coli*, which is also associated with urinary tract infections.

We have added this point to the limitations paragraph of the discussion (paragraph 3). We agree with the reviewer that subscapular inoculation is not a natural mode of transmission. Our focus in the development of the model was to establish a reproducible infection across litters that recapitulates features of human disease and can be used to study the neonatal immune response to infection. We acknowledge this is a model of neonatal sepsis disease syndrome and not a model of natural transmission. This is discussed further in the manuscript.

Authors describe this model as "Early-onset neonatal sepsis" (line 557-558), however their model more resembles "Late onset neonatal sepsis". In short, early onset sepsis occurs within 72hrs of birth, is mostly associated with group B strep, which is thought to be transmitted from the mother to the infant either in utero or during delivery. Late onset sepsis occurs at least 72 hrs post-delivery and the causative bacterial pathogen is community acquired, introduced either from intravenous clinical work or via translocation from the GI tract.

We appreciate the reviewer's point that there is a small discrepancy in the age at which the neonates in our model acquire the infection relative to human neonates diagnosed with EOS. This is, however, minor. In our model the pups are infected on the 3rd day (which can technically fall within 72 h and sometimes does) or 4th day of life. The latter is only up to one day removed, but more important is the administration, trajectory of the infection, and pathogen. LOS is most frequently associated with invasive interventions such as mechanical ventilation and intravascular catheterization, invasion by skin commensals, or dissemination from early colonization of the GI tract. As a responsible pathogen, *E. coli* is significantly outnumbered by coagulase-negative staphylococci (CONS) and *S. aureus* in LOS. Moreover, LOS infections typically develop more slowly in association with biofilm formation and are often accompanied by underlying host conditions or low birth weight status. So, taken together and the minor discrepancy in day of infection aside, we respectfully disagree that this is a model of LOS. However, we thank you for this comment as it is important to distinguish. Although in humans group B *Streptococcus* is the most common etiologic agent, *E. coli* is a very close second. Also important are much higher mortality rates observed with K1-encapsulated *E. coli*, the pathogenic serotype we use in this study. These epidemiologic facts are stipulated in the first paragraph of the Introduction. We look at this mouse infection as a way to model the early human infection and to better understand how the neonatal host responds to early onset pathogens.

Minor Concerns: Protocol 1 (steps 1.5-1.7) Authors should include the target optical density and how that relates to the bacterial concentration they use. Of course target ODs and bacterial concentration are subject to variation in species growth patterns. Since the authors use target concentrations of around 2 to 7×10^6 CFUs, they should have a target OD of the bacterial stock after 2-3 hours.

There is no target OD and we respectfully decline to include since that would be a misrepresentation of our approach. The efficacy of our approach is rooted in a reliable 3 h growth curve that predicts the bacterial density of a 2-3 h culture with minimal variation. Although it is not the focus of the manuscript, we believe strongly that this curve more accurately predicts a bacterial density than a single OD reading. The reason is that target ODs often attempt to manufacture a density with the use of dilution or concentration because it is difficult to naturally stop a bacterial culture to pinpoint a target OD based on time of growth.

Reviewer #3:

Manuscript Summary: Seman et al describe a protocol for performing intravital imaging and various ex vivo analysis of tissues using a gram-negative model of neonatal sepsis. The protocol is clear and would be useful for dissemination to the broader scientific community. There are several instances where their methods could be more detailed and several clarifications that would improve the ease with which other investigators could implement this protocol in their own facility. I have also included several potential suggestions for improving methodology which are meant to be helpful as the authors continue to utilize this approach. These have been highlighted below.

General comments:

1. Please speak to precautions or protocols to maintain body temperature when pups are separated from their dams. At this age, pups are dependent on dams for maintaining body temperature. Example of things to include: Do you use a heat pad? Do you build a nest with bedding materials? Do you give pups back to dams as soon as infection is performed? Are control (uninfected) animals also separated during this time?

Neonates are taken from the dams temporarily for injection, and then immediately placed back with her so they are not given enough time to lose body temperature (now stated in 3.6 and was previously stated in 5.8 of the protocol). Both infected and uninfected controls are

housed together with the mother because all pups are still nursing during the period of infection, though control pup tails are snipped, and both control and infected pup tails are tattooed to individually identify each pup (stated in section 2, Animal Identification).

2. It would be helpful to provide more information about serial dilution technique. For example, what media do you dilute in? How many replicate plates are you using? For recovery from tissue, what controls are used to validate that CFUs are of the inoculated *E. coli* and not endogenous *E. coli* or other bacteria?

Dilutions are done in PBS (neutral pH) containing no calcium or magnesium. Briefly, bacteria are diluted 10-fold are then plated, in duplicate, onto TSA with kanamycin (30 µg/mL) quadrant plates. These plates are incubated at 37°C overnight before enumeration. The mobilized recombinant DNA that contains the lux operon contains a kanamycin resistance cassette. Growth on kanamycin distinguishes the infection strain from endogenous bacteria. We also plate blood or diluted tissue homogenates from control animals and find that there is no colony growth at any dilution or undiluted in tissues of uninfected mice. These details have been added.

3. There is not enough information detail regarding the materials used. Please go through the manuscript and make sure the materials section reflect what was described above. To start, here is an incomplete list of materials required that were not listed: homogenizer, medias, Spectramax plate reader, IVIS intravital imaging machine, real-time thermocycler, formalin, "nylon basket", etc.

This has been completed as requested.

Minor Concerns:

1. Some parts of the technique are described as being performed in a biosafety cabinet hood while others are not. Unless specified, is a biosafety cabinet not required?

We have added to the protocol the other times during which a procedure needs to be done under a biosafety cabinet hood. Generally, procedures such as inoculations of bacteria and necropsy of infected animals should be performed in a biosafety cabinet.

2. For the animal identification protocol, it is unclear if tail snipping and tail tattooing are separate approaches for identification or if all tails are snipped prior to tattoo ink injection. Protocol only says to cut tails of control animals.

Only control animals receive tail snips; infected animals do not. There are only so many unique patterns of tattoo that can be implemented on a neonatal tail. Snipping creates a first layer to uniquely identify. Both control and infected animals receive tail tattoos as an additional layer of identification. This has been clarified in the animal identification section of the protocol.

3. Are both infectious inoculum and PBS control kept on ice until infection?

Yes. This is added to section 3 in the protocol.

4. It would be helpful to explicitly list endpoint criteria in a listed fashion under its own subheading under Section 4. How much body weight loss triggers endpoint?

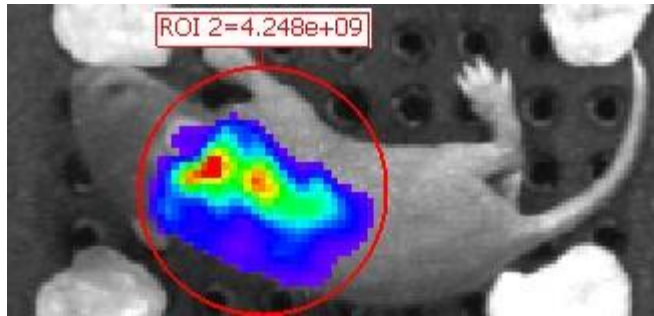
5. For in vitro assay, please include more detail about mixing and centrifugation of samples. Are samples centrifuged prior to removing media before adding gentamycin?

Samples do not need to be centrifuged prior to removing media as they are plated on cell-culture treated plates and adhere to the bottom of the dish. Media is gently pipetted out of the well and gentamicin-supplemented media is gently added back in. This is now clarified in step 12.13.

6. It might also be helpful to include images of the ROI measurement and subsequent data representation.

This is relatively minor and the instructions are pretty straight forward. This image may help demonstrate. This is a representative image of a mouse with the ROI luminescence

quantified (24 h). At the Reviewer or Editor's request we could include as a figure, but it seems an unnecessary use of figure space.



Potential areas for methodological improvements:

1. The current described approach to anesthesia could be further optimized to prevent adverse effects from direct inhalation of isoflurane soaked cotton balls. The discussion brings up another idea of using This reviewer would recommend incorporating a transparent isoflurane chamber that is directly compatible with imaging and using continuous flow through that container during imaging to maintain a consistent and safe amount of isoflurane throughout the entire imaging process. This could be accomplished by purchasing a pre-made manifold made for this purpose (<https://www.environmental-expert.com/products/patterson-five-mouse-imaging-chamber-677727>) or creating one in house.

Thank you for the suggestion. Our system has a continuous flow isoflurane delivery system, but due to the reduced inhalation with neonates, it is less effective.

2. There have been several previous reports using longitudinal intravital imaging after oral administration of bioluminescent bacteria in murine neonates to study the kinetics of bacterial dissemination. PMIDs for reference are 15774831, 25210785, 26351276, 31700190. That does not discount the utility of this protocol, but I would like to refer the authors to this previous work on the topic if they were not already aware of it.

Thank you for raising our awareness to these studies.